OPEN

Quantification of β-Cell Mass in Intramuscular Islet Grafts Using Radiolabeled Exendin-4

Daniel Espes, MD,[1,2] Ramkumar Selvaraju, PhD,[3] Irina Velikyan, PhD,[3,4] Martin Krajcovic, MSc,[3] Per-Ola Carlsson, MD, PhD,[1,2] Olof Eriksson, MSc, PhD[3,5]

Background. There is an increasing interest in alternative implantation sites to the liver for islet transplantation. Intramuscular implantation has even been tested clinically. Possibilities to monitor β-cell mass would be of huge importance not only for the understanding of islet engraftment but also for the decision of changing the immunosuppressive regime. We have therefore evaluated the feasibility of quantifying intramuscular β-cell mass using the radiolabeled glucagon like peptide-1 receptor agonist DO3A-VS-Cys^{40}-Exendin-4. **Methods.** One hundred to 400 islets were transplanted to the abdominal muscle of nondiabetic mice. After 3 to 4 weeks, 0.2 to 0.5 MBq [^{177}Lu]DO3A-VS-Cys^{40}-Exendin-4 was administered intravenously. Sixty minutes postinjection abdominal organs and graft bearing muscle were retrieved, and the radioactive uptake measured in a well counter within 10 minutes. The specific uptake in native and transplanted islets was assessed by autoradiography. The total insulin-positive area of the islet grafts was determined by immunohistochemistry. **Results.** Intramuscular islet grafts could easily be visualized by this tracer, and the background uptake was very low. There was a linear correlation between the radioactivity uptake and the number of transplanted islets, both for standardized uptake values and the total radiotracer uptake in each graft (percentage of injected dose). The quantified total insulin area of surviving β cells showed an even stronger correlation to both standardized uptake values ($R = 0.96$, $P = 0.0002$) and percentage of injected dose ($R = 0.88$, $P = 0.0095$). There was no correlation to estimated α cell mass. **Conclusions.** [^{177}Lu]DO3A-VS-Cys^{40}-Exendin-4 could be used to quantify β-cell mass after experimental intramuscular islet transplantation. This technique may well be transferred to the clinical setting by exchanging Lutetium-177 radionuclide to a positron emitting Gallium-68.

(*Transplantation Direct* 2016;2: e93; doi: 10.1097/TXD.0000000000000598. Published online 22 July 2016.)

Since the introduction of the Edmonton protocol in 2000, the outcome after islet transplantation has dramatically improved and is now a potential curative treatment for selected patients with type 1 diabetes.[1] However, despite improved short-term results, the long-term results are still discouraging, and most of the patients return to an insulin-dependent state after a few years.[2] In addition, the insulin-independent patients exhibit an insulin secretory capacity that averages only 25% of that in healthy individuals already 1 year posttransplantation.[3] By performing intravenous glucose and arginine challenge tests, the functional β cell mass can be estimated; however, this is both time-consuming and challenging for the patient and therefore not suitable as a continuous follow-up procedure. Hence, in clinical practice, the islet graft function is routinely monitored by after the patient's plasma glucose and C-peptide concentrations and exogenous insulin needs. Because there is currently no established method for quantifying the number of surviving islets after transplantation, there are no means to adapt the immune therapy to signs of rejection and declining islet mass.

Many of the challenges in islet transplantation are linked to the liver as implantation site, including substantial cell death early after implantation[4] (caused by an instant blood mediated inflammatory reaction),[5] low oxygenation,[4,6] poor revascularization,[7,8] high concentrations of toxic drug metabolites,[9] and amyloid formation.[10,11] Due to these challenges,

Received 22 February 2016. Revision requested 8 April 2016.

Accepted 28 April 2016.

[1] Department of Medical Cell Biology, Uppsala University, Sweden.

[2] Department of Medical Sciences, Uppsala University, Sweden.

[3] Division of Molecular Imaging, Department of Medicinal Chemistry, Uppsala University, Sweden.

[4] PET Center, Uppsala University Hospital, Sweden.

[5] Turku PET center, Faculty of Natural Sciences and Technology, Åbo Akademi, Turku, Finland.

This work received financial support from the Swedish Research Council (55X-15043), the Swedish Juvenile Diabetes Foundation, the Swedish Diabetes Foundation and the Novo Nordisk Foundation.

The authors declare no conflicts of interest.

D.E., P.-O.C., and O.E. designed the study. D.E., P.-O.C., and O.E. analyzed data and wrote the article. D.E., R.S., and O.E. performed the animal experiments. I.V. performed the radiochemistry experiments. M.K. analyzed data. All authors have reviewed and approved the article for submission.

Correspondence: Daniel Espes, MD, Department of Medical Cell Biology, Uppsala University, Box 571, SE-75123, Uppsala, Sweden. (daniel.espes@mcb.uu.se).

ISSN: 2373-8731

DOI: 10.1097/TXD.0000000000000598

there is an increasing interest in alternative implantation sites. In the experimental setting, many organs have been investigated including muscle,[12-16] omentum,[17-19] bone marrow,[20] spleen,[21] kidney capsule,[21-23] pancreas,[24,25] and the anterior chamber of the eye.[26,27] Experimental studies have shown that islets transplanted to muscle have a superior function and revascularization when compared with islets transplanted to the intraportal site.[12,13] In addition, the intramuscular site has been evaluated in the clinical setting for autologous islet transplantation.[13,28]

The liver also constitutes a major challenge for quantifying and assessing the islet graft from a monitoring point-of-view. First of all, it is almost impossible to harvest representative biopsies containing islets from the liver. Moreover, none of the currently available imaging modalities, ultrasonography, computed tomography, and magnetic resonance imaging have a high enough resolution to discern single islets. In contrast, in a composite islet graft in the forearm muscle magnetic resonance imaging has successfully been used to visualize the graft.[13]

Glucagon-like peptide-1 receptor (GLP-1R) has been shown to be highly expressed in human and murine islets of Langerhans, and to be almost specific to β cells.[29] Exendin-4, a potent GLP-1R agonist radiolabeled with gamma emitting Indium-111 could visualize islets transplanted to muscle in mice as well as in a human subject by single photon emission computed tomography (SPECT).[28,30] However, SPECT lacks the absolute quantification capability required for a more exact measurement of the number of islets in a graft or in the pancreas. Labeling of the Exendin-4 probe with the positron emitting nuclide Gallium-68 was thus performed, and the resulting positron emission tomography (PET) ligand [^{68}Ga] Ga-DO3A-VS-Cys^{40}-Exendin4 has been used for quantitative imaging of the pancreas in several species including human.[31-33] Conveniently, [^{177}Lu]-DO3A-VS-Cys^{40}-Exendin-4, with its longer half-life (6 days), behaves very similar with respect to biodistribution and β cell targeting in vitro and in vivo.[34,35]

In the current study, we investigated the feasibility of quantifying the specific signal from pancreatic β cells and the total number of surviving β cells at the intramuscular site using the GLP-1R agonist DO3A-VS-Cys^{40}-Exendin-4–labeled with Lutetium-177.

MATERIALS AND METHODS

Animals

All experiments were approved by the regional animal ethical board of Uppsala University. Male C57BL/6 mice weighing approximately 25 g were purchased from Taconic (Ry, Denmark). All animals were housed under standardized conditions with ad libitum access to food and water.

Mouse Islet Isolation and Culture

Pancreatic islets were isolated using collagenase digestion and density gradient purification.[8] Islets were cultured overnight in RPMI1640 medium (Sigma-Aldrich, Irvine, UK) supplemented with L-glutamine (2 mmol/L; Sigma-Aldrich), benzylpenicillin (100 U/mL; Roche Diagnostics, Mannheim, Germany) and 10% (vol/vol) fetal calf serum.

Islet Transplantation

On the day of transplantation, 100 to 400 islets were manually counted and handpicked; islets with central necrosis and/or a damaged capsule were discarded. Animals were anesthetized with an intraperitoneal injection of Avertin (0.02 mL/g), a 2.5% solution of 10 g 97% 2.2.2-tribromoethanol (Sigma-Aldrich) in 10-mL 2-methyl-2-buthanol (Kemila, Stockholm, Sweden). In all animals (n = 12), 2 islet grafts were transplanted (n = 24 islet grafts, see Table 1). A midline incision was made in the skin, and the abdominal muscle was exposed. Syngeneic islets were infused into the muscle at both the left and right sides using a butterfly needle (25G). In each case, the infused volume was 100 to 120 μL.

Radiochemistry

Auxiliary material files may require downloading to a local drive depending on platform, browser, configuration, and size. To open auxiliary materials in a browser, click on the label. To download, Right-click and select "Save Target As…" (PC) or CTRL-click and select "Download Link to Disk" (Mac).

Additional file information is provided in the readme.txt.

Hydrochloric acid solution of $^{177}LuCl_3$ (100 μL, 0.1 mol/L; IDB, Holland, BV) of 4.6 GBq was buffered with sodium acetate buffer (200 μL, 1 mol/L pH 4.6). An aqueous solution of DO3A-VSCys^{40}-Exendin-4 (25 μL, 1 mmol/L), and 99.5% ethanol (200 μL) was added, and the reaction mixture was incubated for 15 minutes at 75°C. Purification was carried out by solid phase extraction on a disposable hydrophilic-lipophilic-balanced cartridge, and 50% ethanol was used for the product recovery. Then, ascorbic acid was added as radical scavenger to suppress radiolysis. The product was kept at –20°C until used. A quality control was conducted using reverse phase separation by high-performance liquid chromatography with UV detectors and radiodetectors.[24] The specific radioactivity of [^{177}Lu] Lu-DO3A-VS-Cys^{40}-Exendin-4 was 140 MBq/nmol at the end of the synthesis.

Ex Vivo Organ Distribution Studies

Mice (n = 10) were administered 0.2 to 0.5 MBq [^{177}Lu] DO3A-VS-Cys40-Exendin-4 intravenously in the tail vein, corresponding to 0.82 ± 0.18 μg/kg of [^{177}Lu]DO3A-VS-Cys40-Exendin-4. Two separate mice received a higher dose of [^{177}Lu]DO3A-VS-Cys40-Exendin-4 to assess if the binding in the grafts could be competed (5-7 MBq corresponding to 10.8-16.5 μg/kg). All animals were euthanized by CO_2 60 minutes postinjection of tracer.

Blood, heart, lungs, liver, pancreas, spleen, kidney, intramuscular islet grafts, urinary bladder, subcutaneous fat, muscle, bone, and small and large intestines (without content) were harvested immediately post mortem, weighed and measured for radioactivity in a well-counter within 10 minutes for all animals (Uppsala Imanet; GE Healthcare, Uppsala, Sweden). The radioactive uptake was corrected for the time

TABLE 1.

Description of number of islets transplanted to each animal

Animal												
	Baseline										Competition	
	1	2	3	4	5	6	7	8	9	10	11	12
Left graft	400	400	400	400	400	400	300	300	300	200	400	400
Right graft	200	200	200	200	200	200	100	100	200	200	200	200

of injection and expressed as standardized uptake value (SUV) (according to equation 1) to be comparable between individuals.

$$SUV = \frac{Radioactivity_{organ}(MBq) \times weight_{mouse}(g)}{Radioactivity_{injected}(MBq) \times weight_{organ}(g)} \quad (1)$$

Additionally, the total radiotracer uptake in each graft was assessed as the percentage of injected dose (%ID) by calculating the total uptake in muscle biopsies containing islet grafts ($Bq/cc_{graft} \times$ Graft biopsy weight) and subtracting the calculated background concentration in a pure muscle biopsy with identical weight ($Bq/cc_{muscle} \times$ graft biopsy weight). This was performed to reduce the signal dilution effect caused by the muscle tissue, which would not be present during in vivo scanning.

Autoradiography

After the ex vivo organ distribution studies, the pancreas and intramuscular grafts of each animal were either directly frozen or fixed in formalin and embedded in paraffin. Sections from frozen tissue were prepared on the same day as the experiment, whereas paraffin embedded tissue was sectioned consecutively and evaluated by autoradiography within 6 days (the half-life of Lutetium-177). Autoradiography experiments were performed both for baseline (n = 10) and competition (n = 2) studies. Ten microliters of a Lutetium-177 reference with known radioactivity was included on a separate object glass to enable quantification of islet uptake in Bq/pixel and consequently fmol because the specific radioactivity in fmol/Bq is known. After exposure, each phosphor screen was scanned by using a Cyclone phosphorimage (PerkinElmer, Waltham, MA). Acquired images were analyzed using ImageJ (NIH, Bethesda, MD). When evaluating images with ImageJ software, Rainbow RGB was used as lookup table, and regions of interest were drawn manually around the islet grafts and the native islets by using selection brush tool. Regions of interest were also drawn in exocrine pancreatic tissue and muscle tissue surrounding the islet grafts. References were measured in a gamma well counter and used to quantify the tracer uptake per islets ($fmol/mm^3$).[26]

Immunohistochemistry

Paraffin-embedded islet grafts (n = 8) were consecutively sectioned, and every other section was stained for insulin (guinea pig polyclonal; dilution 1:400; Fitzgerald, Acton, MA), detected by MACH 3 Rabbit HRP-Polymer Detection (Biocare Medical, Concord, CA) and visualized by 3,3′-diaminobenzidine.[36] The insulin area was determined manually using a Leica LMD6000-microscope (Leica Microsystems, Wetzlar, Germany). The total area of the islet graft was calculated as an area under the curve by plotting the known areas.

Sections were double-stained for insulin (Fitzgerald) and glucagon (mouse monoclonal, dilution 1:800; Abcam, Cambridge, UK) with Alexa Fluor 488 (goat anti-guinea pig) and Alexa Fluor 594 (donkey antimouse; dilution 1:250; Invitrogen, Carlsbad, CA) as secondary antibodies. Images were acquired with Zeiss LSM780 (Zeiss, Jena, Germany) confocal. The area of insulin and glucagon was determined with the image software Imaris (Bitplane AG, Zurich, Switzerland). The estimated total α cell area was calculated by multiplying the α cell percentage with the total insulin area for the respective islet graft.

Statistical analysis

Graph Pad Prism version 6.07 (GraphPad Software, La Jolla, CA) was used for statistical analysis. A paired 2-tailed *t* test was applied for comparison between 2 groups. Correlations were calculated by Pearson correlation coefficient. Normality distribution of data was evaluated by Shapiro-Wilk normality test. *P* values less than 0.05 were considered statistically significant. All values are given as mean ± SEM.

RESULTS

Ex Vivo Biodistribution

Muscle biopsies containing the islet grafts had a significantly higher uptake than the muscle background ($P < 0.001$ and $P < 0.01$, respectively) (Figure 1A). The pure muscle biopsy uptake was close to 0 (SUV < 0.1). There was major uptake and retention in the lungs, pancreas, kidneys, and urine.

Coinjection of greater than 10 μg DO3A-VS-Cys^{40}-Exendin-4 together with the tracer competed away the binding in tissues containing β cells, pancreas, and intramuscular islet grafts, indicating GLP-1R–specific mediated binding (Figure 1B). Binding in GLP-1R–negative tissues such as liver was not decreased by coinjection of greater than 10 μg DO3A-VS-Cys^{40}-Exendin-4.

There was a linear correlation between the radioactivity uptake and the number of transplanted islets, both when measuring the concentration (SUV, Figure 1C) and the total radiotracer uptake in each graft (%ID) (Figure 1D). However, there were overlaps between groups, probably due to differences in β cell survival in the islet grafts.

When computing correlations for the grafts in which the total insulin area of surviving β cells was determined (n = 8 islet grafts), a correlation coefficient for SUV of 0.96 ($P = 0.0002$) (Figure 1E) and 0.88 ($P = 0.0095$) for %ID (Figure 1F) was observed.

Ex Vivo Autoradiography

Autoradiograms of mouse pancreas showed that the [^{177}Lu]DO3A-VS-Cys40-Exendin-4 binding was located primarily in the pancreatic islets of Langerhans (Figure 2A). The intramuscularly transplanted islets were readily identifiable from the muscle background in the graft containing biopsies (Figures 2B-C).

The receptor density in islets was approximately 3.5 times higher than the exocrine background ($P < 0.0001$, Figure 2D). The islet-to-background contrast was even higher in muscle, approaching 40 times higher binding ratio ($P < 0.0001$). Importantly, there was unaltered binding between pancreatic and transplanted islets both when expressed as binding density ($fmol/mm^3$ islet tissue) and as binding per islet equivalent (data not shown).

The total amount of bound ligand in each graft was estimated by multiplying the fmol bound per islet equivalent in each graft with the total amount of islets transplanted (100, 200, 300, or 400). There was a positive linear correlation between total amount of [^{177}Lu]DO3A-VS-Cys40-Exendin-4 (fmol) bound in each graft, and the number of islets transplanted, as assessed by ex vivo autoradiography (Figure 2F). Also,

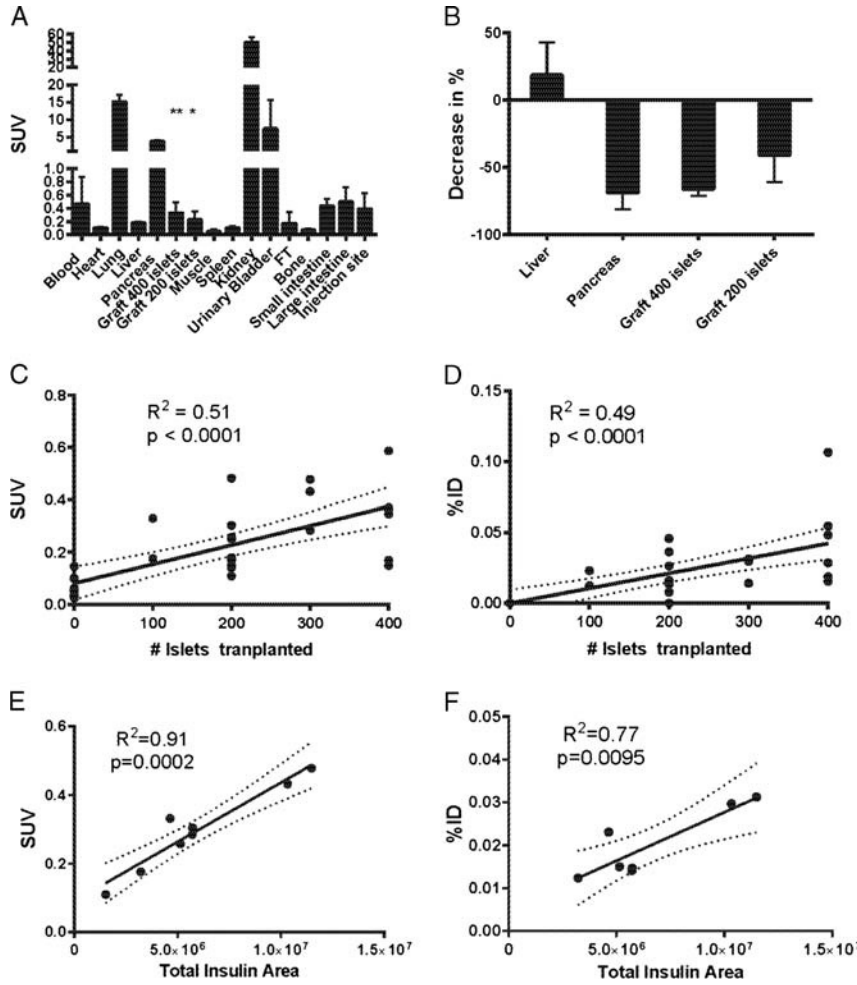

FIGURE 1. A, Biodistribution expressed as SUV (n = 10 animals). B, Competition with greater than 10 μg/kg DO3A-VS-Cys^{40}-Exendin-4 decreased the tracer binding in pancreas (69%), in grafts with 400 islets (66%) and 200 islets (41%) but not in tissues not positive for GLP-1R such as liver (increase 19%). C, Linear correlation between concentration of radioactivity (SUV) measured in each muscle biopsy containing islet graft and the number of islets transplanted. D, Linear correlation between total radioactivity measured in each islet graft, corrected for the background muscle uptake, and the number of islets transplanted. There was a strong positive correlation between the surviving engrafted islets (assessed as insulin positive area in each graft containing muscle biopsy) and the radioactive uptake measured as concentration SUV (E) as well as the total uptake %ID (F).

when computing correlations to the total insulin area of the surviving transplanted islets, a positive correlation was observed (Figure 2G). There was no positive linear correlation between radioactive signal and the estimated total glucagon area (data not shown).

DISCUSSION

In the present study, we found that GLP-1R agonist DO3A-VS-Cys^{40}-Exendin-4 labeled with ^{177}Lu could effectively be used to detect pancreatic islet grafts at the intramuscular site. The intramuscular site is promising for islet imaging, due to the very low islet-to-background signal in muscle. In fact, for this tracer, the ratio was close to 40 which could be compared with a ratio of 3.5 for endogenous islets in the pancreas in relation to exocrine tissue. The intramuscular islet grafts could therefore easily be distinguished from muscle biopsies without transplanted islets.

Interestingly, the [^{177}Lu] Lu-DO3A-VS-Cys^{40}-Exendin-4 binding in each individual islet was similar in transplanted and in native pancreatic islets. This indicates that GLP-1 receptor expression was unaltered in intramuscularly transplanted islets, compared with endogenous islets in mice. As previously reported, the delivery and uptake of the PET tracer are dependent on the revascularization of the islet graft[30] and islets transplanted to muscle have an excellent revascularization and a vascular density comparable to that of endogenous islets.[13,14] However, even at the intramuscular site, the revascularization process is not complete until 14-days post-transplantation, even though the first penetrating vessels can be observed already after 5 days.[13] Therefore, [^{177}Lu] Lu-DO3A-VS-Cys^{40}-Exendin-4 would probably not be useful as a marker of islet mass in the acute setting after islet transplantation.

We observed a strong correlation between the total insulin area of the surviving islet graft and the uptake of [^{177}Lu] Lu-DO3A-VS-Cys^{40}-Exendin-4, both when expressed as SUV and %ID. This was feasible, because the potentially confounding background signal in muscle was negligible.

In the clinical setting, a method for quantifying transplanted β cells would be of tremendous interest, because that would make it possible to monitor the survival of the islet

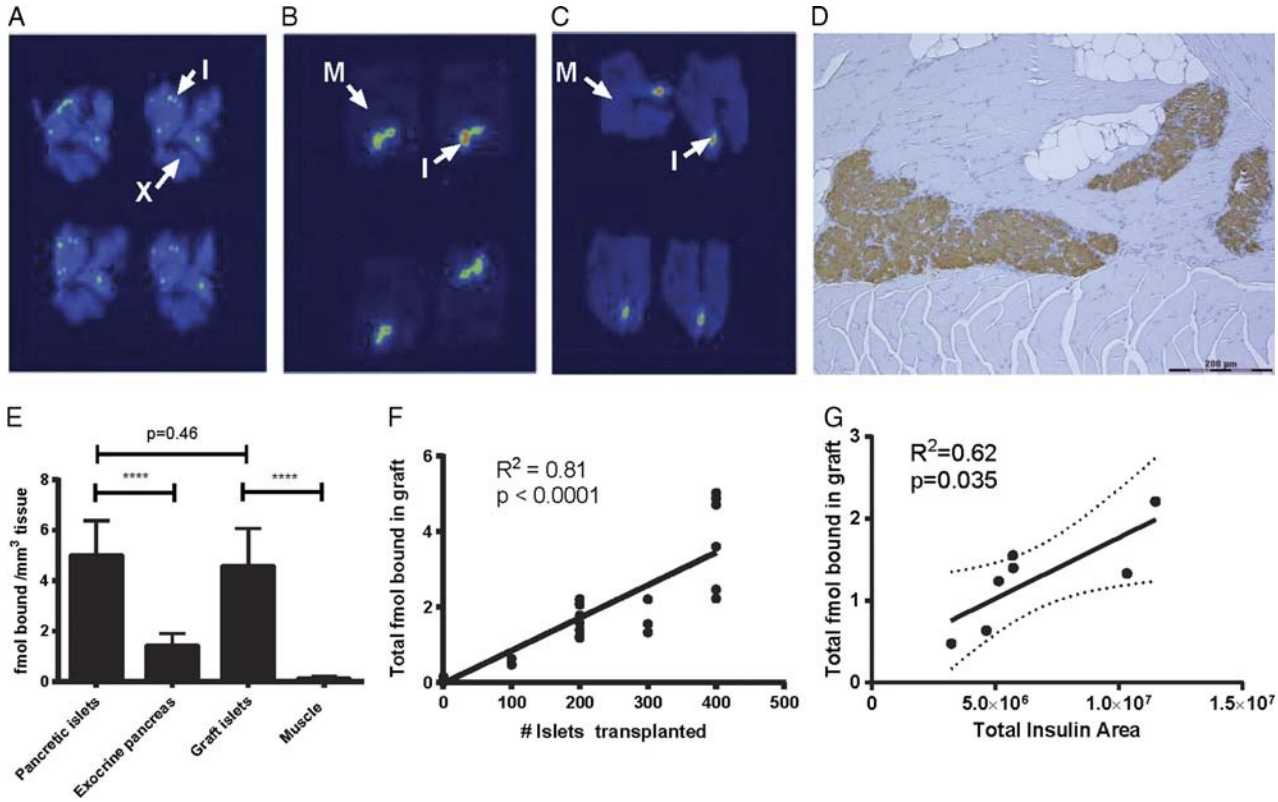

FIGURE 2. Autoradiograms of a representative animal showing 4 consecutive sections of pancreas (A), intramuscular islet graft from an animal transplanted with 400 islets (B) and 200 islets (C). Arrows indicate background of islets. I, islet of Langerhans; X, exocrine pancreas; M, muscle. D, Immunohistochemical staining of paraffin embedded section of an intramuscular islet graft. Insulin stained in brown, counterstaining with hematoxylin. Scale bar represents 200 µm. [^{177}Lu]DO3A-VS-Cys40-Exendin-4 binding was quantified as fmol tracer bound per mm^3 of tissue (E). There was a linear correlation between total amount of fmol [^{177}Lu]DO3A-VS-Cys40-Exendin-4 bound in each graft, as assessed by ex vivo autoradiography, and the number of islets transplanted (F) as well as the total insulin positive area in each graft (G).

graft posttransplantation. In our mouse model, it was possible to detect a difference of about 200 islets, although overlap between the groups remained. However, in the clinical setting, the number of transplanted islets is vastly higher (>10.000 islet equivalents/kg). Based on the quantitative binding data in Figure 2, a clinical islet graft would have the potential of binding an excess of 6 nmol DO3A-VS-Cys^{40}-Exendin-4, given that a similar peptide amount is administered (<1 µg/kg). The clinically significant changes in islet graft mass are in the range of 1000 to 10,000 islets which could, based on the extrapolation above, be detected despite the small total volume of the islet graft without any major problems.

To provide higher image resolution and prolonged monitoring in autoradiography experiments in the present study, we used Lutetium-177 as a convenient replacement nuclide to the positron emitting Gallium-68. It has previously been shown that there is little alteration in biodistribution and islet-specific targeting when changing the radiolabel from Gallium-68 to Lutetium-177.[35] However, when applying this technique in the clinical setting, [^{68}Ga]Ga-DO3A-VS-Cys^{40}-Exendin-4 would be used which would provide advantages such as absolute quantification of the islet graft signal, higher image quality and a lower radiation dose. Additionally, the spatial resolution is higher compared with other radionuclide imaging techniques, such as SPECT. This is of utmost importance in this specific setting, because a graft smaller than the minimum voxel size may lead to significant partial volume effects, potentially underestimating the graft signal. Also, it has been shown that the relatively low radiation dose (due in part to the short half-life of ^{68}Ga but also the low total dose) enables for 2 to 4 repeated examinations yearly in the same individual.[34]

The correlation of the radioactive signal of [^{177}Lu] Lu-DO3A-VS-Cys^{40}-Exendin-4 was related to the insulin positive area and not to glucagon positive area, indicating that [^{177}Lu] Lu-DO3A-VS-Cys^{40}-Exendin-4 had a higher preferential binding to β cells. In a recent study, the uptake of Exendin-4 in α cell was studied in detail in native pancreatic islets and found to be negligible.[29] This is an important aspect for a PET-tracer intended for β cell imaging because the percentage of β cells is highly variable in human pancreatic islets, ranging from 50% to 80% of the islet volume.[37]

By combining PET examinations with Exendin-4 and functional estimates of the islet graft, that is, glucose- and arginine-stimulated measurements of insulin secretion, it would be possible to discern the functional from the anatomical β-cell mass and thereby making it possible to address both β-cell dysfunction in addition to β-cell death posttransplantation.

In conclusion, we provide evidence that the radiolabeled GLP-1R agonist DO3A-VS-Cys^{40}-Exendin-4 can effectively be used to quantify the number of surviving β cells after intramuscular islet transplantation in the experimental setting. The technique may well be transferred to the clinical setting, thereby making it an irreplaceable tool for evaluating β-cell mass in islet transplantation.

ACKNOWLEDGMENTS

Veronica Asplund (Department of Medicinal Chemistry, Uppsala University) is gratefully acknowledged for her expert technical assistance in animal experiments. Dr. Zhanchun Li and Eva Törnelius (Dept. of Medical Cell Biology, Uppsala University) are gratefully acknowledged for their technical assistance and expertise in immunohistochemistry.

REFERENCES

1. Shapiro AM, Lakey JR, Ryan EA, et al. Islet transplantation in seven patients with type 1 diabetes mellitus using a glucocorticoid-free immunosuppressive regimen. *N Engl J Med*. 2000;343:230–238.
2. Barton FB, Rickels MR, Alejandro R, et al. Improvement in outcomes of clinical islet transplantation: 1999–2010. *Diabetes Care*. 2012;35:1436–1445.
3. Keymeulen B, Gillard P, Mathieu C, et al. Correlation between beta cell mass and glycemic control in type 1 diabetic recipients of islet cell graft. *Proc Natl Acad Sci U S A*. 2006;103:17444–17449.
4. Eriksson O, Eich T, Sundin A, et al. Positron emission tomography in clinical islet transplantation. *Am J Transplant*. 2009;9:2816–2824.
5. Bennet W, Sundberg B, Groth CG, et al. Incompatibility between human blood and isolated islets of Langerhans: a finding with implications for clinical intraportal islet transplantation? *Diabetes*. 1999;48:1907–1914.
6. Olsson R, Olerud J, Pettersson U, et al. Increased numbers of low-oxygenated pancreatic islets after intraportal islet transplantation. *Diabetes*. 2011;60:2350–2353.
7. Lau J, Carlsson PO. Low revascularization of human islets when experimentally transplanted into the liver. *Transplantation*. 2009;87:322–325.
8. Henriksnas J, Lau J, Zang G, et al. Markedly decreased blood perfusion of pancreatic islets transplanted intraportally into the liver: disruption of islet integrity necessary for islet revascularization. *Diabetes*. 2012;61:665–673.
9. Shapiro AM, Gallant HL, Hao EG, et al. The portal immunosuppressive storm: relevance to islet transplantation? *Ther Drug Monit*. 2005;27:35–37.
10. Westermark P, Eizirik DL, Pipeleers DG, et al. Rapid deposition of amyloid in human islets transplanted into nude mice. *Diabetologia*. 1995;38:543–549.
11. Westermark GT, Westermark P, Berne C, et al. Widespread amyloid deposition in transplanted human pancreatic islets. *N Engl J Med*. 2008;359:977–979.
12. Svensson J, Lau J, Sandberg M, et al. High Vascular density and oxygenation of pancreatic islets transplanted in clusters into striated muscle. *Cell Transplant*. 20;2010:783–788.
13. Christoffersson G, Henriksnas J, Johansson L, et al. Clinical and experimental pancreatic islet transplantation to striated muscle: establishment of a vascular system similar to that in native islets. *Diabetes*. 2010;59:2569–2578.
14. Espes D, Lau J, Quach M, et al. Cotransplantation of polymerized hemoglobin reduces beta-cell hypoxia and improves beta-cell function in intramuscular islet grafts. *Transplantation*. 2015;99:2077–2082.
15. Weber CJ, Hardy MA, Pi-Sunyer F, et al. Tissue culture preservation and intramuscular transplantation of pancreatic islets. *Surgery*. 1978;84:166–174.
16. Lund T, Korsgren O, Aursnes IA, et al. Sustained reversal of diabetes following islet transplantation to striated musculature in the rat. *J Surg Res*. 2010;160:145–154.
17. Yasunami Y, Lacy PE, Finke EH. A new site for islet transplantation—a peritoneal-omental pouch. *Transplantation*. 1983;36:181–182.
18. Jacobs-Tulleneers-Thevissen D, Bartholomeus K, Suenens K, et al. Human islet cell implants in a nude rat model of diabetes survive better in omentum than in liver with a positive influence of beta cell number and purity. *Diabetologia*. 2010;53:1690–1699.
19. Bartholomeus K, Jacobs-Tulleneers-Thevissen D, Shouyue S, et al. Omentum is better site than kidney capsule for growth, differentiation, and vascularization of immature porcine beta-cell implants in immunodeficient rats. *Transplantation*. 2013;96:1026–1033.
20. Cantarelli E, Melzi R, Mercalli A, et al. Bone marrow as an alternative site for islet transplantation. *Blood*. 2009;114:4566–4574.
21. Korsgren O, Jansson L, Andersson A, et al. Reinnervation of transplanted pancreatic islets. A comparison among islets implanted into the kidney, spleen, and liver. *Transplantation*. 1993;56:138–143.
22. Carlsson PO, Palm F, Andersson A, et al. Chronically decreased oxygen tension in rat pancreatic islets transplanted under the kidney capsule. *Transplantation*. 2000;69:761–766.
23. Carlsson PO, Palm F, Andersson A, et al. Markedly decreased oxygen tension in transplanted rat pancreatic islets irrespective of the implantation site. *Diabetes*. 2001;50:489–495.
24. Stagner JI, Rilo HL, White KK. The pancreas as an islet transplantation site. Confirmation in a syngeneic rodent and canine autotransplant model. *JOP*. 2007;8:628–636.
25. Lau J, Kampf C, Mattsson G, et al. Beneficial role of pancreatic microenvironment for angiogenesis in transplanted pancreatic islets. Cell Transplant. 2009;18:23–30
26. Perez VL, Caicedo A, Berman DM, et al. The anterior chamber of the eye as a clinical transplantation site for the treatment of diabetes: a study in a baboon model of diabetes. *Diabetologia*. 2011;54:1121–1126.
27. Abdulreda MH, Caicedo A, Berggren PO. Transplantation into the anterior chamber of the eye for longitudinal, non-invasive in vivo imaging with single-cell resolution in real-time. *J Vis Exp*. 2013;73:e50466.
28. Pattou F, Kerr-Conte J, Wild D. GLP-1-receptor scanning for imaging of human beta cells transplanted in muscle. *N Engl J Med*. 2010;363:1289–1290.
29. Brom M, Joosten L, Frielink C, et al. (111)In-exendin uptake in the pancreas correlates with the beta-cell mass and not with the alpha-cell mass. *Diabetes*. 2015;64:1324–1328.
30. Eter WA, Bos D, Frielink C, et al. Graft revascularization is essential for non-invasive monitoring of transplanted islets with radiolabeled exendin. *Sci Rep*. 2015;5:15521.
31. Nalin L, Selvaraju RK, Velikyan I, et al. Positron emission tomography imaging of the glucagon-like peptide-1 receptor in healthy and streptozotocin-induced diabetic pigs. *Eur J Nucl Med Mol Imaging*. 2014;41:1800–1810.
32. Selvaraju RK, Velikyan I, Johansson L, et al. In vivo imaging of the glucagonlike peptide 1 receptor in the pancreas with 68Ga-labeled DO3A-exendin-4. *J Nucl Med*. 2013;54:1458–1463.
33. Eriksson O, Velikyan I, Selvaraju RK, et al. Detection of metastatic insulinoma by positron emission tomography with [(68)ga]exendin-4-a case report. *J Clin Endocrinol Metab*. 2014;99:1519–1524.
34. Selvaraju RK, Bulenga TN, Espes D, et al. Dosimetry of [(68)Ga]Ga-DO3A-VS-Cys(40)-Exendin-4 in rodents, pigs, non-human primates and human—repeated scanning in human is possible. *Am J Nucl Med Mol Imaging*. 2015;5:259–269.
35. Velikyan I, Bulenga TN, Selvaraju R, et al. Dosimetry of [(177)Lu]-DO3A-VS-Cys(40)-Exendin-4—impact on the feasibility of insulinoma internal radiotherapy. *Am J Nucl Med Mol Imaging*. 2015;5:109–126.
36. Ullsten S, Lau J, Carlsson PO. Vascular heterogeneity between native rat pancreatic islets is responsible for differences in survival and revascularisation post transplantation. *Diabetologia*. 2015;58:132–139.
37. In't Veld P, Marichal M. Microscopic anatomy of the human islet of Langerhans. *Adv Exp Med Biol*. 2010;654:1–19.